ChinaRxiv

AI translation · View original & related papers at
chinarxiv.org/items/chinaxiv-202201.00018

Improved formation density measurement using controllable D-D neutron source and its lithological correction for porosity prediction

Authors: Zhang, Li, Yu, Hua-Wei, Li, Yang, Jia, Wen-Bao, Han, Xiao, Geng, Xue-Sen, Li, Yang

Date: 2021-12-31T14:48:26+00:00

Abstract

Controllable D-D neutron sources offer long service life, low cost, and no radioactivity. They show favorable prospects for application in geophysical well logging, as traditional chemical radioactive sources used in well logging pose potential safety hazards to human health and the environment. This paper presents an improved method for measuring formation density using a D-D neutron source. Additionally, the lithological effect on density measurements was eliminated to better estimate formation porosity. First, we investigated the spatial distribution of capture gamma rays through Monte Carlo simulations, as well as the relationship between the ratio of capture gamma-ray counts and formation density, to provide theoretical support for the design of density logging tools and their corresponding data processing methods. Second, we obtained the far-to-near detector count ratio of capture gamma rays for an optimized tool structure and established its correlation with the density and porosity of three typical formations composed of pure quartz, calcite, and dolomite minerals. Third, we determined correction values for the densities of sandstone and dolomite relative to limestone at the same porosity and established equations for calculating these correction values, which provides a solid foundation for accurate formation porosity calculation. We observed that capture gamma-ray counts first increased and then decreased, varying across different formations, particularly in high-porosity formations. Under the same lithologic conditions (rock matrix), as porosity increases, the peak of the gamma-ray count distribution shifts toward the neutron source. At different detector-source distances, the ratio of capture gamma-ray counts exhibited a strong correlation with formation density. A formation density conversion equation was established based on the ratio of capture gamma-ray counts at detector-source distances of 30 cm and 65 cm, and the calculated values agreed well with the true values. After correction, the formation density values showed excellent agreement with the

true limestone density values, with a mean absolute error of -0.013 g/cm^3. The calculated porosity values were very close to the true values, with a mean relative error of 2.33%, demonstrating the accuracy of the proposed method. These findings provide a new approach for developing D-D neutron source logging tools and their corresponding well-log data processing methods.

Full Text

Improved Formation Density Measurement Using a Controllable D-D Neutron Source and Its Lithological Correction for Porosity Prediction

Li Zhang[1],[4], Hua-Wei Yu[2], Yang Li[3],*, Wen-Bao Jia[4], Xiao Han[1], Xue-Sen Geng[1]

[1]School of Geosciences, China University of Petroleum, Qingdao 266580, China
[2]College of Mechanical & Electronic Engineering, Shandong Agricultural University, Tai' an 271018, China
[3]Department of Nuclear Science and Engineering, Nanjing University of Aeronautics and Astronautics, Nanjing 211106, China
*Corresponding author, mtlyab@sdau.edu.cn

Abstract: Controllable D-D neutron sources offer long service life, low cost, and non-radioactive operation, presenting favorable prospects for geophysical well logging applications. Traditional chemical radioactive sources used for well logging pose potential threats to human safety and the environment. This paper presents an improved method for measuring formation density that employs a D-D neutron source, along with a technique to remove lithological effects for better porosity estimation. First, we investigated the spatial distribution of capture gamma rays through Monte Carlo simulations and established the relationship between the ratio of capture gamma ray counts and formation density, providing theoretical support for density logging tool design and data processing methods. Second, we obtained the far-to-near detector count ratios for an optimized tool structure and established its correlation with the density and porosity of three typical formations composed of pure quartz, calcite, and dolomite minerals. Third, we determined correction values for sandstone and dolomite densities relative to limestone data at equivalent porosity and established equations for calculating these correction values, laying a solid foundation for accurate formation porosity calculation. We observed that capture gamma ray counts initially increased then decreased, with variations across different formations, particularly in high-porosity formations. Under the same lithologic conditions (rock matrix), as porosity increases, the peak gamma ray count moves toward the neutron source. At different detector-source distances, the ratio of capture gamma ray counts correlated well with formation density. A formation density conversion equation was established based on the ratio of capture gamma ray counts at detector-source distances of 30 cm and 65 cm, and the calculated values showed excellent agreement with true values. After correction, the forma-

tion density was highly consistent with the true limestone density, with a mean absolute error of -0.013 g/cm^3. The calculated porosity values were very close to the true values, with a mean relative error of 2.33%, highlighting the accuracy of the proposed method. These findings provide a new approach for developing D-D neutron source logging tools and their associated data processing methods.

Keywords: Density measurement; D-D Neutron Source; Lithological correction; Porosity prediction

Introduction

Density logging is an effective method for porosity determination and lithology identification. With the development of geophysical prospecting for fossil fuels, density logging theories and methods have become increasingly important in recent years [**?**, **?**]. In particular, growing awareness of health, safety, and environmental concerns has necessitated the use of alternative sources in density logging [**?**]. Several research institutions and scholars both in China and abroad have investigated replacing chemical sources with D-T neutron [**?**] and X-ray sources [**?**, **?**] in density logging, and progress has been made in establishing density measurement and correction methods [**?**]. D-D neutron sources are superior to D-T neutron sources, offering advantages of long service life, low cost, and non-radioactivity [**?**, **?**]. However, the relatively low neutron yield of D-D sources has historically restricted their development [**?**, **?**].

In recent years, with increasing neutron yields from D-D sources, their application in well logging has attracted greater attention [**?**, **?**]. D-D neutron sources can produce high thermal neutron fluxes through interaction with formations and are typically used directly in neutron porosity logging [**?**], but their application in density logging remains in the exploration stage. He et al. analyzed the energy spectra of γ-rays generated by D-D neutron source-formation interactions and found that both capture γ-ray and mixed-field γ-ray spectra correlated well with formation density [**?**]. Zhang Li studied the feasibility of using D-D neutron sources in density logging and investigated factors affecting the spatial distribution of induced gamma rays [**?**, **?**]. Some Chinese companies and institutes, such as China Oilfield Services Limited, have conducted studies on density logging with controllable D-D neutron sources and noted that the spatial distribution of induced γ-rays significantly impacts logging tool design [**?**]. While previous studies verified the feasibility of density measurement with controllable D-D neutron sources, detailed methods for density calculation and correction were not provided.

Building upon previous research, this study proposes a method for measuring formation density with a D-D neutron source and correcting for lithological effects. The Monte Carlo N-Particle Transport Code (MCNP) was used to investigate the characteristics of capture gamma ray spatial distribution across various formation lithologies, analyze the relationship between gamma ray count ratios and formation density at different detector-source distances, and establish

equations for calculating formation density. Finally, using limestone data as a reference, density correction values were determined under varying porosity conditions, providing a solid foundation for accurate porosity calculations. This study offers a reference for developing controllable D-D neutron source density logging tools and researching their applications.

1. Theoretical Background

During D-D source density logging, the pulsed neutron generator (nuclear reaction formula: $\langle MATH_0 \rangle$) generates 2.45 MeV fast neutrons that react with formation nuclides. The γ-rays produced during these reactions serve as the induced γ-ray source for measuring formation density. It has been verified that the induced γ-rays are primarily capture γ-rays. Unlike the point γ-ray sources used in traditional density logging, capture γ-rays are not monoenergetic, and their spatial positions are not fixed. The photons from these spatially distributed capture γ-rays constitute the γ-ray source for density logging. After generation, capture γ-rays undergo attenuation. The γ-ray flux measured by detectors can be calculated as [**?**, **?**]:

$$\langle MATH_1 \rangle$$

where $\langle MATH_2 \rangle$ is the neutron flux, $\langle MATH_3 \rangle$ is the γ-ray mass attenuation coefficient, and $\langle MATH_4 \rangle$ is the bulk density of the formation.

Equation (1) indicates that detector responses to capture γ-rays depend on the formation' s macroscopic capture cross-section, thermal neutron distribution, and formation density. Consequently, the ratio of capture gamma ray counts measured by gamma-ray detectors may vary even in formations with identical density, primarily because capture gamma ray counts are affected by both the macroscopic capture cross-section and the spatial distribution of thermal neutrons. Figure 1 shows the distribution of capture gamma ray fluxes in three formations (sandstone, limestone, and dolomite) with the same density ($\langle MATH_5 \rangle$). Capture gamma ray flux intensity is color-coded (high values in red, low values in blue).

Fig. 1 (Color online) Distributions of capture gamma ray flux in three formations (sandstone, limestone, and dolomite) with the same density.

As shown in Fig. 1, in the three formations with identical density, gamma rays exhibit distinct spatial distribution patterns in zones around the neutron source. The capture gamma ray flux varies significantly near the far detector, as demonstrated by different color distributions and ranges in the blue area shown in the right panels of Fig. 1. The capture gamma ray flux was lowest in dolomite and highest in sandstone. Using gamma ray counts from a single detector to determine formation density introduces significant measurement errors.

To eliminate the effects of other factors on density measurement, we used the

ratio of capture γ-ray counts measured by two detectors (near and far) to determine formation density. The relationship between this ratio, denoted as R, and formation density can be derived from Eq. (1):

$$\langle MATH_6 \rangle$$

where $\langle MATH_7 \rangle$ and $\langle MATH_8 \rangle$ are the distances from the near and far detectors to the neutron source, respectively, and $\langle MATH_9 \rangle$ and $\langle MATH_{10} \rangle$ denote the neutron flux measured by the near and far detectors, respectively. R is primarily related to formation density but is also affected by the spatial distribution of neutrons. This study focuses on calculating density using the ratio of gamma-ray counts measured by the two detectors.

In nuclear logging, the Monte Carlo method is commonly employed to study particle reaction processes and spatial distributions. MCNP is a general-purpose Monte Carlo particle transport code capable of simulating various particles, including neutrons, photons, and electrons [**?**, **?**]. In this study, we used this method to investigate capture gamma ray spatial distribution characteristics under various formation conditions. We constructed a pure theoretical model (excluding wellbore and logging instruments), as shown in Fig. 2, consisting of a sphere divided into numerous concentric spherical shells with a radial increment of 5 cm. The initial radius (detector-source distance) is $r = 5$ cm, and the outermost sphere radius is $r = 120$ cm.

The neutron source is located at point O, the sphere' s center, with neutrons emitted directly into the formation. Gamma ray fluxes through the spherical surfaces are recorded. The D-D neutron generator yield is 1×10^7 n/s, with a neutron source energy of 2.45 MeV.

Fig. 2 (Color online) Calculation model.

Three typical formations—sandstone, limestone, and dolomite—were used for simulation. The rock matrices were SiO_2, $CaCO_3$, and $CaMg(CO_3)_2$, respectively. The pore fluid was H_2O, with porosity varying from 0–40% in 2% increments. Detailed parameters are listed in Table 1.

Table 1 Parameter information of three typical lithologic strata.

Lithology	Rock Matrix	Pore Fluid	Porosity (%)	Density (g/cm^3)
Sandstone	SiO_2	H_2O	0–40	Variable
Limestone	$CaCO_3$	H_2O	0–40	Variable
Dolomite	$CaMg(CO_3)_2$	H_2O	0–40	Variable

The calculation model shown in Fig. 2 was used to record gamma-ray fluxes through spherical surfaces under various formation conditions (as listed in Table

1), yielding gamma-ray counts at different detector-source distances. The results are presented in Fig. 3.

Fig. 3 (Color online) Distribution of capture gamma rays in three different lithologic strata with varying source distances: (a) Sandstone formation, (b) Limestone formation, (c) Dolomite formation.

Figure 3 shows that as detector-source distance increases, gamma ray counts initially increase then decrease, with the distribution range affected by porosity. For pure minerals with zero porosity, capture gamma rays exhibited a wide spatial distribution range. As porosity increased, the spatial distribution range narrowed, and the peak gamma ray count moved toward the neutron source. At 40% porosity, the peak value was closest to the neutron source.

The primary reason is that water serves as the pore fluid in numerical simulations. High porosity indicates high hydrogen content, causing neutrons to slow down rapidly. With more thermal neutrons in zones near the neutron source, the gamma ray count from thermal neutron capture increases. Note that thermal neutron counts are also affected by other formation elements such as carbon, silicon, and magnesium. In low-porosity formations, the effects of these elements are not negligible. In pure rock matrices, neutrons slow down over longer distances, so when they become thermal neutrons, they are farther from the neutron source, causing the peak capture gamma ray count to also be farther from the source. The spatial distribution pattern of capture gamma rays varies across formations, closely related to the elements in different rock matrices.

2. Relationship Between the Ratio of Capture Gamma Ray Counts and Formation Density

We analyzed gamma ray counts measured in different formations at various detector-source distances to determine the optimal ratio for density calculation. As shown in Fig. 3, peak captured γ-ray counts in different formations were primarily distributed within 20–80 cm. Peak locations represent the main distribution zones of capture gamma rays. We analyzed the relationship between capture gamma ray count ratios and formation density through fitting at various detector-source distances. The results in Table 2 show that for formations with the same lithology, the capture gamma ray count ratio was highly correlated with formation density, with an average correlation coefficient of 0.99.

Table 2 Correlation coefficient of the counting ratio and formation density under 42 different source distance combinations.

Detector Spacing	Sandstone	Limestone	Dolomite
20/50	···	···	···
20/55	···	···	···
···	···	···	···

Detector Spacing	Sandstone	Limestone	Dolomite
45/80	···	···	···

The above analysis demonstrates that within the main gamma capture spatial distribution area (20–80 cm from the neutron source), gamma count ratios under various source distance combinations correlated well with formation density, particularly when the near-source distance was 25–35 cm and the far-source distance was 50–70 cm. Additionally, practical instrument dimensions, including detector size and shield thickness, must be considered. After comparison, near and far source distances of 30 cm and 65 cm were selected. Based on this structural design, a logging instrument model was developed, as shown in Fig. 4.

Model parameters are as follows: wellbore diameter of 20 cm filled with fresh water; D-D neutron source yield of 2×10^7 n/s with 40 s pulse width; two NaI-type gamma-ray detectors positioned 30 cm (near) and 60 cm (far) from the D-D neutron source, with lengths of 5 cm and 10 cm, respectively; tungsten-iron-nickel shields (density 17.78 g/cm^3) placed between the neutron source and detectors and between the near and far detectors.

Fig. 4 (Color online) Schematic diagram of instrument model.

Using the model in Fig. 4, we obtained near-to-far detector gamma ray count ratios in sandstone, limestone, and dolomite formations with varying porosity (parameters listed in Table 1) and analyzed the relationship between count ratios and formation density, as shown in Fig. 5.

Fig. 5 (Color online) Relationship between capture gamma ray count ratio and formation density for the source distance combination of 30/65 cm.

The density calculation equations for the three formations were determined to be:

Sandstone: $\langle MATH_{11} \rangle$, $R^2 = 0.9976$
Limestone: $\langle MATH_{12} \rangle$, $R^2 = 0.9947$
Dolomite: $\langle MATH_{13} \rangle$, $R^2 = 0.9952$

where x_c is the capture gamma count ratio between near and far detectors, and y_d is formation density.

Figure 5 and Eqs. (3)-(5) show that in all three formations, the relationship between gamma ray count ratio and formation density follows a functional form. As the gamma ray count ratio increases, formation density decreases, with the ratio affected by formation porosity. Higher porosity yields higher gamma ray counts in both near and far detectors because increased hydrogen content slows neutrons more rapidly, increasing thermal neutron flux near the near detector and the number of gamma rays from thermal neutron capture. Consequently, the gamma ray count measured by the far detector decreases with increasing

porosity, causing the near-to-far count ratio to increase. While the gamma ray count ratio fits formation density well in all three formations, lithological effects are significant and must be corrected to obtain accurate formation density information.

3. Method for Correcting Lithology Effects

Formation density data are frequently used in geophysical prospecting to determine porosity. However, precise transformation of density data to porosity is challenging because density is strongly affected by mineral composition. Inaccuracies in matrix density significantly impact calculated porosity. To accurately determine formation porosity, density logs must typically be converted to values relative to a standard lithology to eliminate the impact of improperly selected matrix parameters on calculation results.

First, we calculated densities of sandstone, limestone, and dolomite formations with varying porosities using the formation density equations. Second, we computed lithology correction values for the three formations across different porosities. The results are shown in Table 3.

Table 3 Three lithologic and stratigraphic density corrections.

Porosity (%)	Sandstone Density (g/cm^3)	Limestone Density (g/cm^3)	Dolomite Density (g/cm^3)	Correction Values
...	...	...	...	...

Table 3 shows that different correction values are needed for lithology effects on density in formations with varying porosity. The calculated sandstone formation density was slightly higher than true values, while dolomite formation density was slightly lower. Therefore, lithology correction values are negative for sandstone and positive for dolomite. We analyzed the relationship between porosity and corresponding correction values for these three formations, as shown in Fig. 6. The fitted equations are:

Sandstone: $\langle MATH_{14} \rangle$, $R^2 = 0.9733$
Limestone: $\langle MATH_{15} \rangle$, $R^2 = 0.9802$
Dolomite: $\langle MATH_{16} \rangle$, $R^2 = 0.9859$

where x_p is porosity and Δy_d is the density correction value.

Figure 6 shows that density correction values correlate well with porosity for all three formations. The limestone formation exhibited the smallest correction values due to statistical errors, while the dolomite formation showed large correction values ($ 0.16g/cm^{3}$ for porosity <40%). The sandstone formation showed moderate correction values that decreased with increasing porosity,

reaching 0.0122 g/cm^3 at 40% porosity. Using these correction values, formation porosity can be accurately calculated to quantitatively determine formation parameters.

Fig. 6 (Color online) Density corrections for sandstone, limestone, and dolomite for different porosity.

To validate the accuracy of density measurements and lithology correction effects on porosity, we calculated densities and porosities of sandstone, limestone, and dolomite formations (with water as pore fluid) at porosities of 3%, 5%, 13%, 15%, 23%, 25%, 33%, and 35% using Monte Carlo numerical simulation and the model shown in Fig. 4. The calculated values were compared with theoretical values, as shown in Figs. 7 and 8.

Fig. 7 (Color online) Relationship between calculated and true density values obtained using the density fitting formula.

Figure 7 shows that nearly all density values calculated using the density equations fall on the 45° line, demonstrating high consistency with true values and verifying equation accuracy. Lithology significantly impacts calculated density values, and these measurement errors affect porosity calculations.

Fig. 8 (Color online) Comparison of calculated and true porosity values before and after correction: (a) Sandstone, (b) Dolomite.

Fig. 9 (Color online) Relative error of calculated porosity before and after correction.

Figure 8 compares sandstone and dolomite formation porosities calculated before and after lithology correction. Before correction, porosity values are distributed on both sides of the 45° line, with dolomite data points farther from the line. After correction, calculated porosity values show high consistency with true values, with most falling on the 45° line. Figure 9 shows relative errors in calculated porosity for sandstone and dolomite. For porosity <5%, relative errors are significant but <5%, except for sandstone where the error reaches 30% due to cumulative density measurement errors. For porosity >5%, relative errors in calculated porosity are <4%, demonstrating correction method effectiveness. Formation porosity parameters obtained from D-D neutron source density measurements show that lithology effects are non-negligible, particularly in low-porosity formations, and must be corrected to obtain accurate formation parameters.

4. Conclusion

In density measurements with a D-D neutron source, lithology significantly impacts the spatial distribution of capture gamma rays. In formations with the same lithology, capture gamma ray spatial distribution follows predictable patterns, while varying lithologies produce substantially different distributions.

Analysis using a neutron source-formation model revealed that for porosity ranging 0–40%, capture gamma rays in the three typical formations are primarily distributed 20–80 cm from the neutron source.

Formation density can be determined using the ratio of gamma ray counts measured by two gamma-ray detectors. The capture gamma ray count ratio was highly correlated with formation density, with a correlation coefficient of 0.99. However, density measurement was affected by lithology, requiring different equations for density calculation in formations with varying lithologies.

The accuracy of the formation density calculation equations and lithology correction methods was verified using simulation data. The mean error of density values obtained from the calculation equations was <0.015 g/cm^3, satisfying density measurement requirements. After lithology correction, the mean relative errors in calculated formation porosity were $<4\%$, demonstrating that the proposed correction method effectively reduces lithology effects on porosity calculation and improves formation parameter accuracy.

Author Contributions

All authors contributed to study conception and design. Material preparation, data collection, and analysis were performed by Li Zhang, Hua-Wei Yu, Yang Li, Wen-Bao Jia, Xiao Han, and Xue-Sen Geng. The first draft was written by Li Zhang, and all authors commented on previous versions. All authors read and approved the final manuscript.

Funding

This work was partly supported by the National Natural Science Foundation of China (Nos. 41704113, 41674129), Key R&D Projects in Shandong Province (No. 2019GSF109047), China Postdoctoral Science Foundation Grant (No. 2019M661912), and Science and Technology Plan Project of Shandong Education of China (Nos. J18KA190 and J18KA128).

References

1. M. Evans, R. Adolph, L. Vildé et al., *A sourceless alternative to conventional LWD nuclear logging.* SPE Annual Technical Conference and Exhibition, Dallas, Texas, October 2000, SPE 62982-MS (2000). https://doi.org/10.2118/62982-MS

2. H. Peng, *Review on progress of radioactive well logging technology in 2000-2008.* Well Logging Technol. 33(1) 1-8 (2009). https://doi.org/10.16489/j.issn.1004-1338.2009.01.008 (in Chinese)

3. J.D. Aitken, R. Adolph, M. Evans et al., *Radiation sources in drilling tools: comprehensive risk analysis in the design, development and operation of LWD tools.* SPE International Conference on Health, Safety and

Environment in Oil and Gas Exploration and Production, March 20-22 (2002). https://doi.org/10.2118/73896-MS

4. A. Badruzzaman, S. Bames, F. Bair et al., *Radioactive sources in petroleum industry: applications, concerns and alternatives*. Asia Pacific Health, Safety, Security and Environment Conference, 4-6 (2009). https://doi.org/10.2118/123593-MS

5. Non-isotopic alternative technologies working group. *Non-Radio isotopic alternative technologies white paper*. U.S. Department of Homeland Security Cybersecurity and Infrastructure Security Agency (2019).

6. R.D. Wilson, *Bulk density logging with high-energy gammas produced by fast neutron reactions with formation oxygen atoms*. In: Proceeding of Nuclear Science Symposium and Medical Imaging Conference, San Francisco (1995). https://doi.org/10.1109/NSSMIC.1995.504211

7. R.C. Odom, D.E. Tiller, R.D. Wilson, *Improvements in a through-casing pulsed-neutron density log*. SPE Annual Technical Conference and Exhibition, New Orleans, Louisiana, September 2001, SPE-71742-MS (2001). https://doi.org/10.2118/71742-MS

8. H.W. Yu, J.M. Sun, J.X. Wang et al., *Accuracy and borehole influences in pulsed neutron gamma density logging while drilling*. Appl. Radiat. Isot. 69, 1313–1317 (2011). https://doi.org/10.1016/j.apradiso.2011.04.023

9. F. Zhang, Y.F. Li, Y. Xin et al., *Numerical simulation of density logging based on X-ray and gamma ray sources*. Journal of China University of Petroleum, 42(01), 60-66 (2018). https://doi.org/10.3969/j.issn.1673-5005.2018.01.007

10. H.W. Yu, X.H. Chen, Y. Zhou et al., *Impact of photoelectric effect on X-ray density logging and its correction*. Appl. Radiat. Isot. 156, 108785 (2020). https://doi.org/10.1016/j.apradiso.2019.06.031

11. B.Z. Pan, R. Zhang, K. Liu et al., *Numerical simulation of pulsed neutron source density logging' s secondary capture gamma ray strength*. Geophysical prospecting for petroleum, 53(6), 642-648 (2014). https://doi.org/10.3969/j.issn.1000-1441.2014.06.003 (in Chinese)

12. F. Zhang, Q.Y. Zhang, J.T. Liu et al., *A method to describe inelastic gamma field distribution in neutron gamma density logging*. Appl. Radiat. Isot. 129, 189-195 (2017). https://doi.org/10.1016/j.apradiso.2017.08.024

13. H.W. Yu, Y.X. Zhang, X.H. Chen et al., *Numerical simulation and method study of X-ray litho-density logging*. Nucl. Sci. Tech. 31(12), 124 (2020). https://doi.org/10.1007/s41365-020-00778-7

14. Z.-W. Huang, J.-R. Wang, Z. Wei et al., *Development of a compact D-D neutron generator*. J. Instrum. 13(1), P01013 (2018). https://doi.org/10.1088/1748-0221/13/01/P01013

15. Y. Gong, X.C. Guan, Q. Wang et al., *Design of moderator for boron neutron capture therapy based on D-D neutron source*. Nucl. Tech. 43(9): 090303 (2020). https://doi.org/10.11889/j.0253-3219 (in Chinese)

16. L. Bond, K. Denslow, J. Griffin, et al., *Evaluation of non-nuclear techniques for well logging technology evaluation*. Washington: PNNL. (2010). https://doi.org/10.2172/1006309

17. J. Griffin, T. Moran, L. Bond, *Radiation source replacement workshop*. Washington: PNNL. (2010) https://doi.org/10.2172/1062523

18. C.R. Peeples, M. Mickael, R.P. Gardner, *On replacing Am-Be neutron sources in compensated porosity logging tools*. Appl. Radiat. Isot. 68(4-5), 926-931(2010). https://doi.org/10.1016/j.apradiso.2009.11.042

19. A.X. Chen, A.J. Antolak, K.-N. Leung, *Electronic neutron sources for compensated porosity logging*. Nucl. Instrum. Meth. A 684, (2012). https://doi.org/10.1016/j.nima.2012.04.053

20. F. Zhang, C. Yuan. *Monte Carlo simulation on compensated neutron porosity logging with D-D neutron generator*. Well Logging Techno. 34(3), 227-232 (2010). https://doi.org/10.16489/j.issn.1004-1338.2010.03.004. (in Chinese)

21. Y. Yan, B.Y. Li, S.P. Zheng et al., *Monte Carlo simulation of the neutron porosity logging using D-D neutron generator*. J Lanzhou Univ (Natural Sciences). 48(03), 123-127 (2012). https://doi.org/10.13885/j.issn.0455-2059.2012.03.009 (in Chinese)

22. A. Badruzzaman, A. Schmidt, A. Antolak et al., *Neutron generator as alternatives to Am-Be source in well logging: An assessment of fundamentals*. Petrophysics. 60(1),136-170 (2019). https://doi.org/10.30632/PJV60N1-2019a10

23. X.Y. He, D.P. Xu, Q. Xie et al., *Monte Carlo simulation of n-γ density logging of D-D neutron generator*. Nucl. Phys. Rev. 30(02), (2013). https://doi.org/10.11804/NuclPhysRev.30.02.151 (in Chinese)

24. L. Zhang, H.W. Yu, *Effect of density measurement on D-D induced gamma counting*. Nucl. Tech. 39(3), 030502 (2016). https://doi.org/10.11889/j.0253-3219.2016.hjs.39.030502 (in Chinese)

25. L. Zhang, H.W. Yu, W.B. Jia et al., *Study on the influence of formation factors on spatial distribution of D-D induced γ-ray source*. Nucl. Tech. 42(1): 010501 (2019). https://doi.org/10.11889/j.0253-3219 (in Chinese)

26. L. Zhang, H.W. Yu, W.B. Jia et al., *A research on the effects of formation elements on the spatial distribution of D-D induced γ-ray source*. Appl. Radiat. Isot. 151, 289-298 (2019). https://doi.org/10.1016/j.apradiso.2019.06.007

27. X.G. Han, R. Pemper, T. Tutt et al., *Environmental corrections and system calibration for a new pulsed-neutron mineralogy instrument*. SPWLA

50th Annual Logging Symposium, 21-24, (2009).

28. F. Zhang, *Foundations of nuclear geophysics*. (Petroleum industry press, Beijing, 2015). (in Chinese)
29. R.P. Gardner, L. Xu, *Status of the Monte Carlo library least-squares (MCLLS) approach for non-linear radiation analyzer problems*. Radiat. Phys. Chem. 78(10), 843-851 (2009). https://doi.org/10.1016/j.radphyschem.2009.04.023
30. T.B. Yang, M. Wang, X.Y. Fan et al., *MCNP simulation for gamma-ray buildup factors of shielding material*. Nucl. Tech. 44(3): 030503 (2021). https://doi.org/10.11889/j.0253-3219 (in Chinese)

Figures

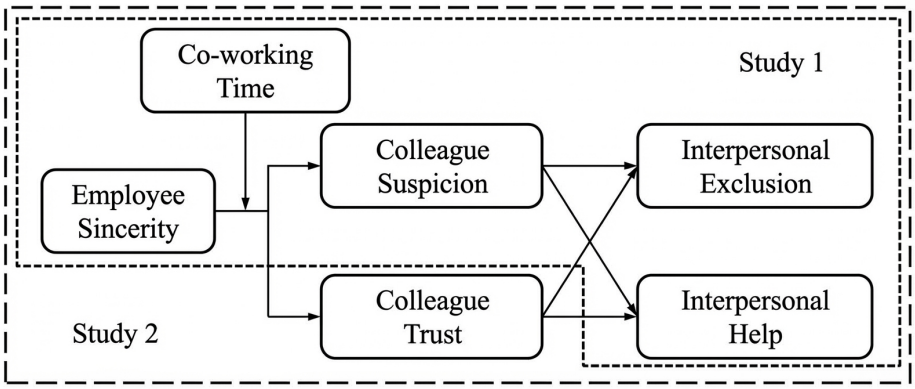

Figure 1: Figure 1

Source: ChinaXiv —Machine translation. Verify with original.